Italian Journal of Food Science, 2025; 37 (1): 220–233

Citral, a major component of lemon myrtle (*Backhousia citriodora*) essential oil, inhibits adipogenesis in 3T3-L1 preadipocytes during mitotic clonal expansion

Yae Rim Choi[1,3], Min Kyung Park[2], Ae Sin Lee[1], Young-Suk Kim[3], Min Jung Kim[1]*

[1]Research Group of Aging and Metabolism, Korea Food Research Institute, Wanju, Republic of Korea; [2]Research Group of Food Processing, Korea Food Research Institute, Wanju, Republic of Korea; [3]Department of Food Science and Engineering, Ewha Womans University, Seoul, Republic of Korea

***Corresponding Author**: Min Jung Kim, Korea Food Research Institute, Wanju-gun, Jeollabuk-do 55365, Republic of Korea. Email: mjkim14@kfri.re.kr

Academic Editor: Prof. Tommaso Beccari, Università degli Studi di Perugia, Italy

Received: 27 July 2024; Accepted: 26 November 2024; Published: 1 January 2025

ORIGINAL ARTICLE

Abstract

Lemon myrtle essential oil (LMEO), a popular food-flavoring and perfume, has anti-inflammatory and antioxidant properties, and contains citral in abundance. Citral-enriched essential oils exhibit anti-obesity effects; however, the effect of LMEO on adipogenesis and the precise mechanism of citral have not been elucidated. This study evaluated the anti-adipogenic activity of commercial LMEO and its components, geranial, neral and citral (a mixture of geranial and neral), in 3T3-L1 cell differentiation and identified the anti-adipogenic mechanism of citral. Treatment of 3T3-L1 preadipocytes with various concentrations of LMEO, neral, geranial, and citral for 24 h and 48 h showed that LMEO (12.5–25 μg/mL) inhibited 3-isobutyl-1-methylxanthine, dexamethasone, and insulin (MDI)-induced differentiation of preadipocytes. Citral, accounting for 88.67% of total compounds in LMEO, also suppressed MDI-induced differentiation and expression of adipogenic transcription factors (*PPARγ*, *C/EBPα*, and *Fabp4*). Additionally, citral inhibited the early stages of differentiation, particularly mitotic clonal expansion (MCE), by deactivating cell cycle-related factors (cyclins and cyclin-dependent kinases) and arresting the cell cycle at G_0/G_1 phase, which was caused by inhibiting upstream signaling pathways, especially PI3K/AKT pathway. Therefore, regulation of early stages of adipogenesis, especially MCE, is a key mechanism underlying the anti-adipogenic activity of citral. LMEO and citral can be potentially used as anti-obesity agents.

Keywords: adipogenesis; anti-obesity; citral; lemon myrtle essential oil; mitotic clonal expansion

Introduction

Lemon myrtle (*LM*), native of Australia, belongs to the shrub family Myrtaceae. Lemon-scented LM is widely used as an ingredient in food items, perfumes, and aromatherapy whereas LM essential oils (LMEO) are used as food-flavorings because of their unique aroma and taste (Southwell, 2021). LMEO contains 80–98% citral, a mixture of two main isomeric aldehydes: geranial and neral. This is higher than that found in other lemony essential oils, such as citrus (3–10%) and lemongrass (75%) (Jain and Sharma, 2017; Mukarram *et al.*, 2021; Sultanbawa, 2016). Other minor components of LMEO include β-myrcene, 6-methyl-5-hepten-2-one, (±)-linalool, citronellal, iso-neral (cis-iso citral), iso-geranial (trans-iso citral), and trans-geraniol.

LMEO exhibits various therapeutic properties, including antimicrobial, antifungal, antioxidant, anti-inflammatory, and anticancer activities (Beikzadeh *et al.*, 2020;

 ISSN 1120-1770 online, DOI 10.15586/ijfs.v37i1.2725

Lim *et al*., 2022; Wang *et al*., 2023). Citral also has antibacterial, anti-inflammatory, and antitumor properties (Gonçalves *et al*., 2020; Nordin *et al*., 2020; Shi *et al*., 2016). Moreover, citral has demonstrated anti-obesity effects in animal models and cellular studies by inhibiting accumulation of abdominal fat during diet-induced obesity (Modak and Mukhopadhaya, 2011). Citral, citral dimethyl acetal, and citral diethyl acetal are the main components of lemongrass essential oil, and they suppress lipid accumulation by decreasing lipid uptake and increasing lipolysis in 3T3-L1 adipocytes (Sprenger *et al*., 2022). LMEO, which contains more citral than lemongrass, may have similar effects; however, this has not been reported. Furthermore, the precise mechanism underlying the anti-obesity effect of citral needs to be studied.

Adipogenesis is a process of preadipocyte differentiation into mature adipocytes and involves various changes in gene expression and cell morphology (Harada *et al*., 2016; Rosen and Spiegelman, 2000). 3T3-L1 preadipocytes undergo the following four stages to completely differentiate into adipocytes: growth arrest, mitotic clonal expansion (MCE), intermediate differentiation, and terminal differentiation (Chang and Kim, 2019). Growth-arrested 3T3-L1 preadipocytes are hormonally induced to express transcription factors C/EBPβ and C/EBPδ, which are the members of the CCAAT–enhancer-binding protein (C/EBP) family of transcription factors. C/EBPβ, a key transcriptional activator of the *C/EBPα* and *PPARγ* genes, initiates post-confluent mitosis and clonal expansion immediately upon treatment of preadipocytes with differentiation inducers, facilitating their re-entry into the cell cycle (Guo *et al*., 2015; Tang *et al*., 2003a). During the MCE stage, C/EBPβ stimulates the expression of cyclins and cyclin-dependent kinases (CDKs) in 3T3-L1 preadipocytes, which are essential for cell regeneration. The expression of cyclin D1 and CDK4 and CDK6 complexes is activated during the G_1 phase; cyclin E and CDK2 are activated at the G_1/S boundary, allowing cells to enter the S phase; and cyclin B and CDK1 complexes are regulated during the G_2/M phase (Tang *et al*., 2003b). After multiple rounds of clonal expansion, the preadipocytes re-enter a quiescent state and experience coordinate transcriptional activation of adipogenesis-related genes, *PPARγ* and *C/EBPα*, and their target genes, *FAS* and *Fabp4* (Ahmad *et al*., 2020; Rosen *et al*., 2002). Inhibition of cell cycle re-entry using a DNA synthesis inhibitor prevents adipocyte differentiation, indicating that an active MCE stage is necessary for differentiation process (Patel and Lane, 2000).

In this study, we investigated the effects of LMEO and its major component, citral, on the inhibition of adipogenesis and regulation of adipogenesis-related genes. Thereafter, the stage at which citral influenced the four stages of adipogenesis was analyzed. Finally, the changes in biomarkers related to cell cycle and adipogenesis during MCE were analyzed. To the best of our knowledge, this is the first study demonstrating the inhibition of adipogenesis in 3T3-L1 cells via the inhibition of MCE stage by LMEO and citral.

Materials and Methods

Materials

Dulbecco's modified eagle medium (DMEM), bovine calf serum (BCS), fetal bovine serum (FBS), and penicillin–streptomycin (P/S) were purchased from Gibco (Grand Island, NY, USA). 3-Isobutyl-1-methylxanthine (IBMX), dexamethasone (DEX), insulin, citral, Oil Red O dye, and isopropyl alcohol were purchased from Sigma-Aldrich (St. Louis, MO, USA). LMEO was purchased from Aromalab Co. Ltd. (Gyeonggi-do, South Korea). Neral and geranial compounds were purchased from A2B Chem (San Diego, CA, USA). Antibodies against *C/EBPβ*, *PPARγ*, *C/EBPα*, *Fabp4*, cyclin D1, CDK6, cyclin E1, CDK2, cyclin B, β-actin, anti-rabbit IgG, and anti-mouse IgG horseradish peroxidase (HRP)-linked antibody were purchased from Cell Signaling Technology (Danvers, MA, USA).

Cell culture and differentiation

Mouse 3T3-L1 preadipocytes were purchased from the American Type Culture Collection (ATCC, USA). The cells were grown in high-glucose DMEM supplemented with 10% BCS and 1% P/S at 37°C in 5% CO_2 atmosphere incubator (Thermo Fisher Scientific, IL, USA). Two days after 100% confluency of preadipocyte was achieved (designated as day 0), cells were differentiated using 0.5-mM IBMX, 1-μM DEX, and 1-μg/mL insulin in DMEM with 10% FBS (MDI medium) for 2 days (designated as MDI). On day 2, the MDI medium was replaced with DMEM+10% FBS medium supplemented with 1-μg/mL insulin, and the cells were cultured for 8 days. The medium was changed every 2 days.

Cell viability

Cell viability was measured using a CCK-8 kit (Dojindo, Kumamoto, Japan). 3T3-L1 preadipocytes were seeded in a 96-well plate at a density of 5×10^4 cells/well. The following day, the cells were treated with various concentrations of LMEO, neral, geranial, and citral for 24 h and 48 h at 37°C. Thereafter, CCK-8 solution was added to each well for 2 h at 37°C. The absorbance was measured

at 450 nm (reference wavelength, 650 nm) using a microplate reader (SpectraMax M2, Molecular Device, USA).

Cell counts were determined using trypan blue assay. Preadipocytes were cultured in MDI medium with or without citral, trypsinized, and resuspended in medium containing 0.4% trypsin blue solution (1:1). Viable cell numbers were measured 24 h and 48 h after treatment using a LUNA-II cell counter (Logo Biosystems, Gyeonggi-do, South Korea).

Oil Red O staining

3T3-L1 preadipocytes were seeded in a 12-well plate and differentiated into mature adipocytes. The cells were then rinsed twice with phosphate buffered saline (PBS) and fixed in 4% paraformaldehyde for 15 min. After washing with PBS, the cells were treated with 60% isopropyl alcohol for 5 min. Intracellular lipid droplets were stained with a filtered 0.5% Oil Red O solution for 10 min. After aspirating the remaining Oil Red O solution, cells were rinsed with PBS. Images of the cells stained with Oil Red O were obtained using a microscope, and the quantitative value of Oil Red O was obtained by eluting the intracellular Oil Red O dye with 100% isopropyl alcohol and measuring the absorbance at 500 nm.

Gas Chromatography–Mass Spectrometry (GC-MS)

Solid phase microextraction (SPME) was used to extract volatile compounds from LMEO and citral. LMEO (100 mg) or citral (10 µL) was put into a 20-mL headspace amber vial and divinylbenzene–carboxen–polydimethylsiloxane fiber (DVB/CAR/PDMS, 50/30 µm; Supelco, Bellefonte, PA, USA) was inserted into the headspace of vial for 30 min at 30°C. Volatile compounds were thermally desorbed into the injector port of GC-MS for 5 min at 250°C. A 7890 A GC (Agilent Technologies, Santa Clara, CA, USA) with 5975 C MS (Agilent Technologies) was used to analyze volatile compounds in LMEO and citral. A fused silica capillary column (DB-UIWAX, 30-m length × 0.25-mm i.d. × 0.25-µm film thickness; J & W Scientific, Folsom, CA, USA) was applied to separate the analytes. The flow rate of helium (carrier gas) was 0.8 mL/min and mass spectra were collected in the electron impact (EI) mode at 70 eV and a mass scan range of 35–350 m/z. Oven temperature was maintained 40°C for 5 min and increased to 220°C at a rate of 4°C/min. Inlet and transfer line temperatures were 230°C and 250°C, respectively.

Volatile compounds were identified by comparing retention period and mass spectral data with those of authentic standard compounds and a commercial GC-MS library (Wiley 7.0). The retention index (RI) of each volatile compound was calculated using n-alkanes (C_7–C_{22}). The relative percentage of each volatile compound was calculated by comparing peak area with total area.

Western blot analysis

The cells were washed twice with pre-chilled PBS and lysed in radioimmunoprecipitation assay (RIPA) lysis buffer. Lysates were centrifuged at 12,000×g for 30 min at 4°C, and supernatant was collected. The total protein concentration was measured using a bicinchoninic acid assay (BCA) protein assay kit. The quantified protein samples were denatured by heating at 105°C for 5 min, and equal amount of protein was separated through sodium dodecyl sulfate–polyacrylamide gel electrophoresis (SDS-PAGE) and transferred onto a polyvinylidene fluoride (PVDF) membrane. The membranes were blocked with 5% *bovine serum albumin* (BSA) and incubated with primary antibodies (*C/EBPβ*, *PPARγ*, *C/EBPα*, *Fabp4*, cyclin D1, CDK6, cyclin E1, CDK2, cyclin B, and β-actin) overnight at 4°C. After washing, the membranes were incubated with secondary antibody for 2 h at room temperature. The bands were visualized by enhanced chemiluminescence using X-ray film.

Real-time polymerase chain reaction (RT-PCR)

Total RNA was isolated from the cells using TRIzol reagent (Thermo Fisher Scientific). Reverse transcription was performed using 1 µg of total RNA, Moloney murine leukemia virus (M-MuLV) reverse transcriptase, deoxynucleotide triphosphate (dNTPs), and an oligo (dT) 18 primer. Quantitative RT-PCR was conducted using synthesized complementary DNA and SYBR-green mix. The PCR conditions included 40 cycles of denaturation at 95°C for 15 s, annealing at 60°C for 60 s, and extension at 60°C for 30 s. The primer sequences used in this study are listed in Table 1. Relative mRNA levels were determined using the delta delta Crossing thresholds (ΔΔCt) method and normalized to *18S* gene in mice.

Cell cycle analysis

Preadipocytes, treated with or without 100-µM citral in MDI medium for 16 or 20 h, were harvested, washed with PBS, and fixed in 70% ethanol at -20°C overnight. Thereafter, the cells were centrifuged, washed with PBS, incubated in 500-µL PBS containing 100-µg/mL ribonuclease (RNase) for 30 min at room temperature, and stained with propidium iodide (PI) solution for 10 min at room temperature. A minimum of 10,000 cells per sample were analyzed using a Beckman flow cytometer, and the data were processed using the CytExpert 2.4 software to determine relative cell numbers in the G_0/G_1, S, and G_2/M phases.

Table 1. Primer sequences for RT-PCR.

Gene	Primer sequence (5'-3')
Pparg	F: AAGGATTCATGACCAGGGAGTTCC
	R: GCGGTCTCCACTGAGAATAATG
Cebpa	F: GTGGACAAGAACAGCAACGAGT
	R: AGGCGGTCATTGTCACTGGTCAA
Fabp4	F: GTGGGCTTTGCCACAAGGAAAGT
	R: GGTGATTTCATCGAATTCCACGCC
Cebpb	F: AACAACATCGCGGTGCGCAA
	R: AACAAGTTCCGCAGGGTGCTGA
Ccnd1	F: AAGCAGACCATCCGCAAGCA
	R: GGTAGCAGGAGAGGAAGTTGTT
Cdk6	F: TTTTCAGATGGCCCTTACCTCG
	R: CCACGAAAAAGAGGCTTTCTGC
Ccne1	F: GTCTAAGCCCTCTGACCATTG
	R: TAAGCAGCCAACATCCAGGACG
Cdk2	F: CGAGCACCTGAAATTCTTCTGG
	R: AGAGTCCGAAAGATCCGGAA
Ccnb1	F: GCATCTAAAGTCGGAGAGGT
	R: GGTGTCCATTCACCGTTGTC
Adipoq	F: AGCCGCTTATGTGTATCGCTCAG
	R: CCCGGAATGTTGCAGTAGAACT
Fasn	F: TGGGTTTGGTGAATTGTCTCCG
	R: ACACGTTCATCACGAGGTCATG
Pnpla2	F: GGAACCAAAGGACCTGATGACC
	R: ACATCAGGCAGCCACTCCAACA
Lipe	F: GCTCATCTCCTATGACCTACGG
	R: TCCGTGGATAACAACCAG G
18S	F: GGTGTCCATTCACCGTTGTC
	R: GTAACCCGTTGAACCCCATT

Statistical analysis

All data were presented as mean ± standard deviation (SD) of triplicate experiments. Statistical analyses were performed using the Prism 9.0 software. One-way ANOVA and two-way ANOVA were used to determine the significance of treatment effects and interactions, followed by Dunnett's and Tukey multiple comparison test to identify significant differences between group mean values. Statistical significance was set at $p < 0.05$ and $p < 0.001$.

Results and Discussion

Effect of LMEO on lipid accumulation in 3T3-L1 adipocytes

Prior to investigating the efficacy of LMEO in 3T3-L1 preadipocytes, its cytotoxicity was evaluated to determine appropriate concentration. LMEO was found to significantly reduce the cell viability of preadipocytes at 50–200 μg/mL, but showed no significant cytotoxicity at 6.25–25 μg/mL (Figure 1A). Therefore, in subsequent experiments, ≤25 μg/mL of LMEO was used. Thereafter, the effect of LMEO on 3T3-L1 differentiation was observed by measuring lipid accumulation in 3T3-L1 cells after treatment with LMEO (6.25–25 μg/mL) for 8 days of differentiation. Representative Oil Red O images and quantitative results revealed that 12.5–25 μg/mL of LMEO significantly reduced lipid accumulation (Figure 1B).

Accumulation of excess fat in adipose tissue is a hallmark of obesity, and anti-obesity effects often depend on the ability to limit lipid accumulation (Longo *et al*., 2019). Essential oils have many biological effects, and the anti-obesity effect of lemon-scented essential oils is also known. Lemongrass essential oil suppresses intracellular lipid accumulation and down-regulates adipogenic factors in 3T3-L1 adipocytes (Sprenger *et al*., 2022). Lemon balm essential oil reduces triglyceride concentration in the adipose tissue of type 2 diabetic mice (Chung *et al*., 2010). Lemon essential oil activates sympathetic nerve activity in the white adipose tissue of epididymis, which may increase lipolysis and suppress gain in body weight (Niijima and Nagai, 2003). Similar to other lemon-scented essential oil, LMEO suppresses lipid accumulation during adipocyte differentiation.

Volatile composition of LMEO

Given the common anti-obesity effects of lemon-scented essential oils, we hypothesized that their constituent compounds might be similar. Therefore, we measured the volatile components present in LMEO using GC-MS. Table 2 lists the volatile compounds identified in LMEO, their percentage contents, and RIs. The total chromatogram (TIC) of GC-MS analysis obtained using LMEO is shown in Figure 2. Approximately 97% of the total volatile compounds were identified using GC-MS, and 28 volatile compounds were identified, including 19 terpenes, two alcohols, five benzenes, and two hydrocarbons. Terpenes accounted for 93% of total volatile compounds. Geranial (*E*-citral, 46.18%) and neral (*Z*-citral, 42.49%) were the main volatile components, followed by sulcatone (2.8%), linalool (1.17%), β-caryophyllene (1.06%), and β-citronellol (0.99%). This result aligned with earlier research in which LMEO was found to be rich in monoterpene aldehydes, specifically neral and geranial (Sultanbawa, 2016), corroborating our findings. Additional investigations consistently demonstrated that LMEO is primarily composed of citral, a monoterpene aldehyde, with isomeric forms, including geranial (46.1–60.7%) and neral (32.0–40.9%) (Sultanbawa, 2016). Lemongrass essential

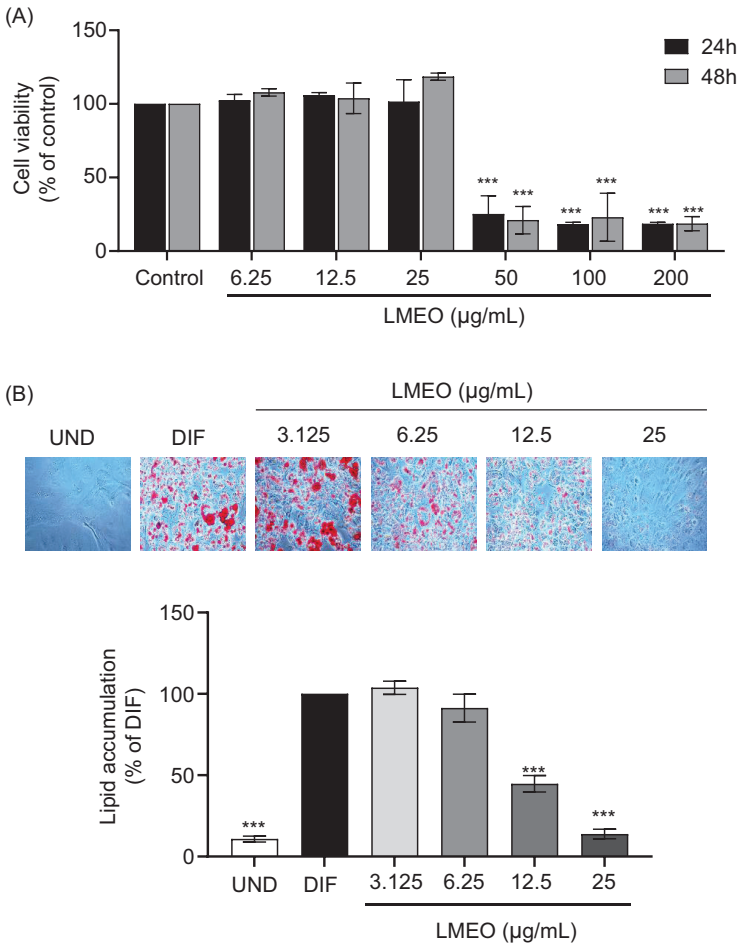

Figure 1. Effects of lemon myrtle essential oil (LMEO) on 3T3-L1 cells. (A) Cytotoxicity of LMEO on 3T3-L1 preadipocytes at 24 and 48 h. (B) Effects of LMEO on adipocyte differentiation of 3T3-L1 cells. After treatment for 8 days, cells were stained with Oil Red O and observed under a light microscope. Lipid accumulation was relatively quantified using Oil Red O staining results. All data are presented as the mean ± SD and analyzed with one-way ANOVA, compared with that from control and DIF group (n ≥ 3, ***$p < 0.001$).

oil includes neral (36.8%) and geranial (42.9%) (Soliman *et al*., 2017). In addition, lemon balm essential oil consists of neral (30.5–31.9%) and geranial (35.6–38.3%) (Ghasemi Pirbalouti *et al*., 2019). Therefore, in this study, geranial and neral were used to investigate the effects of lemon myrtle on adipogenesis.

Effect of citral on lipid accumulation in 3T3-L1 adipocytes

In order to investigate whether the inhibitory function of LMEO on lipid accumulation was due to its major components, preadipocytes were treated with geranial or neral through the same process as LMEO, and lipid accumulation was observed. Geranial and neral treatment were observed to decrease intracellular lipid accumulation in a concentration-dependent manner, especially at 100 μM and 150 μM (Figures 3A and 3B). Citral, a mixture of geranial and neral (Figure 3C) also inhibited intracellular lipid accumulation in a concentration-dependent manner, especially at 50 μM and 100 μM (Figure 3D). In particular, citral exerted a synergistic effect by enhancing its efficacy. The protein and mRNA expressions of *PPARγ*, *C/EBPα*, and *Fabp4*, well-known master regulators of adipocyte differentiation (Moseti *et al.*, 2016), were also affected by citral treatment (Figures 3E–3G). In addition, the mRNA expression levels of *adipoq* and *Fasn,* which are markers of adipokine and lipogenesis, respectively, were reduced by citral (Figure 3G). During differentiation, their expression was up-regulated in the control group (DIF) but was inhibited in the citral-treated group (Figures 3E–3G).

Geranial and neral are structural isomers with similar chemical formulas and functional groups and are naturally occurring compounds found in various essential oils, such as lemongrass, lemon myrtle, and citronella (Mercer and Rodriguez-Amaya, 2021). However, they

Table 2. Composition of volatile compounds identified in lemon myrtle essential oil (LMEO) using GC-MS.

Compound	RI[a]	Area (mean±SD)	RSD (%)	ID[b]
Terpenes				
α-Pinene	1,013	0.01±0.00	11.3	B
β-Pinene	1,099	0.03±0.00	1.8	B
Sabinene	1,115	0.00±0.00	2.6	B
β-Myrcene	1,162	0.15±0.00	2.6	B
α-Terpinene	1,175	0.01±0.00	4.2	B
Limonene	1,193	0.15±0.00	1.3	B
γ-Terpinene	1,242	0.01±0.00	3.3	B
β-Ocimene	1,250	0.02±0.00	1.1	B
o-Cymol	1,267	0.02±0.00	1.7	B
β-Citronellal	1,473	0.99±0.00	0.2	B
α-Copaene	1,485	0.12±0.00	2.0	B
Linalool	1,546	1.17±0.02	1.5	A
β-Caryophyllen	1,590	1.06±0.00	0.4	B
Neral	1,684	42.49±0.07	0.2	A
α-Terpineol	1,698	0.22±0.00	0.9	B
Geranial	1,736	46.18±0.13	0.3	A
β-Citronellol	1,774	0.17±0.01	4.7	A
Nerol	1,802	0.31±0.00	1.3	A
Geraniol	1,852	0.81±0.00	0.1	A
Alcohols				
2-Methylbut-3-en-2-ol	1,039	0.01±0.00	2.4	B
3-Methylbut-2-en-1-ol	1,322	0.09±0.00	1.4	B
Benzenes				
Ethylbenzene	1,120	0.02±0.00	6.1	B
1,4-Xylene	1,126	0.03±0.00	1.8	B
1,3-Xylene	1,134	0.05±0.00	3.4	B
1,2-Xylene	1,178	0.01±0.00	4.6	B
1,2-Diethylbenzene	1,276	0.01±0.00	0.7	B
Hydrocarbons				
6-Methylhept-5-en-2-one	1,334	2.8±0.04	1.5	B
(E)-3-Methylpent-2-ene	1,613	0.1±0.00	2.3	C

[a]RI: Retention indices were calculated using C_6–C_{22} n-alkanes as external standards.
[b]Identification of the compounds was based on the following: A, mass spectrum and retention index agreed with those of standard compounds under the same conditions (positive identification); B, mass spectrum and retention index were consistent with those from the National Institute of Standards and Technology (NIST) library (tentative identification); C, mass spectrum was consistent with that of the W9N08 library (Wiley and NIST) and manual interpretation (tentative identification).

differ in their double-bond configurations, odors, and flavor profiles. Geranial has a trans double-bond between carbons C3 and C4 and is known for its strong lemony, citrus-like aroma and flavor. On the other hand, neral has a cis double-bond between carbons C3 and C4 and has a lemony scent, but is often described as somewhat milder than geranial. These differences have a significant impact on biological efficacy (Araneda *et al*., 2004). Both compounds have an inhibitory efficacy against cytokine expression in murine macrophages (Liao *et al*., 2015), but geranial has a stronger inhibitory effect on tumor growth in p53 null 4T1 breast cancer cells than neral (Zeng *et al*., 2015). The anti-adipogenic effects of geranial and neral were similar, representing a novel finding reported for the first time in this study.

Considering that the mixture of geranial and neral (citral) accounted for 88.67% of the total components, the anti-adipogenic effect of LMEO was presumed to be due to citral. In this study, citral demonstrated a synergistic effect, resulting in more potent inhibition of adipogenesis. Synergy is defined as an interaction between two or more agents that produce a combined effect greater than the sum of their individual effects (Geary, 2013). A combination of grape seed-derived procyanidins and gypenosides had a synergistic effect in reducing relative adipose tissue mass in high-fat diet mice and alleviating insulin resistance (Zhang *et al*., 2009). Additionally, catechins and caffeine, which are components of green tea, synergistically inhibited intracellular fat accumulation in 3T3-L1 cells and reduced body weight gain in mice (Zhu *et al*., 2017). The anti-obesity effects of citral were reported in the past. The main components of lemongrass, namely, citral, citral diethyl acetal, and citral dimethyl acetal, reduced MDI-induced free fatty acid accumulation in 3T3-L1 adipocytes (Sprenger *et al*., 2022). Additionally, citral reduced the level of intracellular triglyceride accumulation and suppressed the expression of adipogenic transcription genes (*PPARγ*, *C/EBPα*, *SREBP-1c*, and *Fas*) in a concentration-dependent manner in 3T3-L1 cells (Sri Devi and Ashokkumar, 2018), which is consistent with our results. Consistently, we found that citral synergistically inhibited the adipogenic process, compared to individual compounds; therefore, the anti-adipogenesis mechanism was estimated using citral.

Inhibition of early adipogenesis in 3T3-L1 preadipocytes by citral

The mechanism of adipogenesis suppression by citral was investigated by treating 3T3-L1 preadipocytes with citral at different time points during the differentiation process (Figure 4A). Oil Red O staining showed that citral significantly inhibited lipid accumulation in cells treated on 0–2, 0–4, and 0–8 days (#1, #2, and #3), compared to the

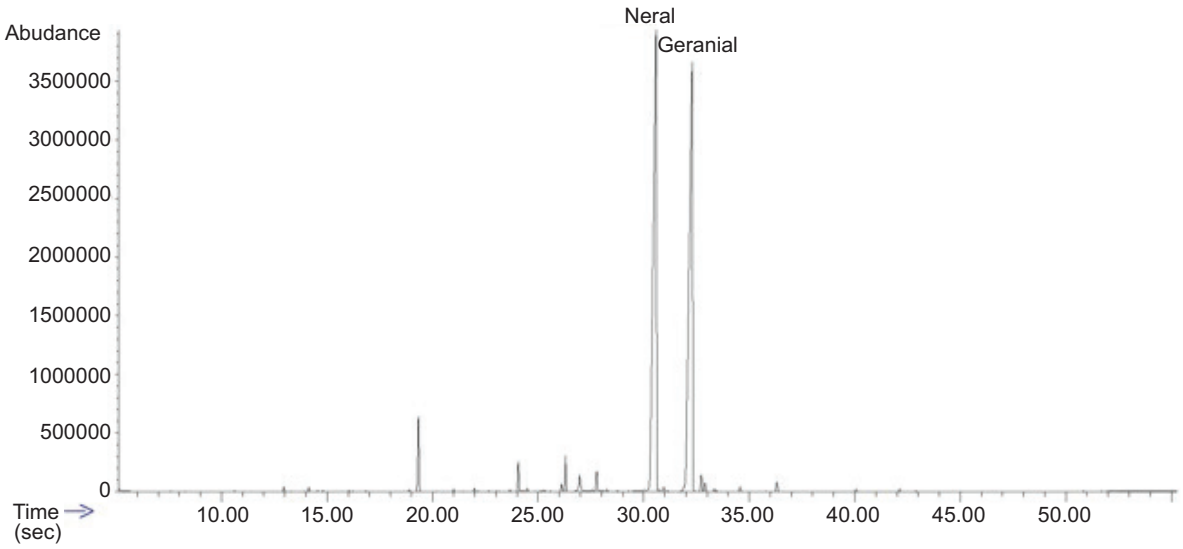

Figure 2. Gas Chromatography–mass spectrometry (GC-MS) chromatogram of LMEO.

control group (DIF) (Figure 4B). However, citral treatment on 2–4 and 4–8 days (#4 and #5) did not suppress intracellular lipid accumulation. This suggested that citral was involved in the early stages of differentiation, that is, 0–2 days (#1). Therefore, changes in differentiation-related markers were examined by comparing #1 and #3. As shown in Figures 4C–4E, the protein and mRNA expression levels of *PPARγ*, *C/EBPα*, and *Fabp4* in #1 and #3 were significantly reduced, compared to those in the control (DIF) group, which was consistent with the Oil Red O staining. In addition, the mRNA expression levels of *Adipoq, Fasn*, and lipolysis markers (*Pnpla2* and *Lipe*) were also reduced effectively by citral. These results indicated that the early stage of differentiation is a critical step in the ability of citral to inhibit adipogenesis.

Adipogenesis is characterized by chronological changes in the expression of various genes that lead to the establishment of adipocyte phenotype (Longo *et al*., 2019). Adipogenesis occurs in multiple stages, including early, intermediate, and terminal differentiation. The number of growth-arrested confluent preadipocytes almost double by day 2 under hormone induction (MCE stage). By day 4, the cytoplasmic triglyceride droplets become visible and accumulate in cells (intermediate stage), and the cells are fully differentiated by day 8 (terminal stage) (Kim *et al*., 2012; Qiu *et al*., 2001; Yu *et al*., 2020). If the MCE of adipogenesis is inhibited, preadipocytes (undifferentiated cells) do not undergo an initial commitment to become mature adipocytes. Therefore, these preadipocytes remain undifferentiated and do not progress onto the next stage of adipogenesis.

Inhibition of the intermediate stage prevents preadipocytes from fully differentiating into mature adipocytes. When this stage is inhibited, preadipocytes are unable to form lipid droplets properly, and the differentiation process is halted. Consequently, the cells may remain in a semi-differentiated state or return to a preadipocyte-like state (Kang *et al*., 2011). Terminal stage inhibition prevents the final maturation of adipocytes, leading to incomplete adipocyte formation. As a result, these cells have reduced lipid storage capacity and impaired function as fully developed adipocytes (Kang *et al*., 2011).

Although the differentiation stage involving citral has not yet been studied, various chemicals have been investigated. Apigenin partially inhibited lipid accumulation and induced a significant 60% reduction in the formation of lipid droplets in 3T3-L1 cells treated during the early stage and almost inhibited lipid accumulation during the early-to-mid (days 0–4) and long-term (days 0–6) stages (Kim *et al*., 2014). *Inula britannica* (IAE) exerted anti-adipogenic effect when applied during the first 2 days of the same 8-day differentiation process as in this experiment, implying the regulation of early stages of adipogenesis (Yu *et al*., 2020). In particular, IAE inhibited MCE by inducing cell cycle arrest at the G_0/G_1 phase and down-regulating MCE-related transcription factors. Early-stage inhibition by citral in this study maintained 3T3-L1 cells in a preadipocyte state, rather than differentiating them into adipocytes. As citral also has the potential to inhibit MCE, similar to IAE, it is necessary to examine its effect on MCE.

Citral-induced suppression of MCE by arresting the cell cycle progression

Mitotic clonal expansion occurs during the early stages of preadipocyte differentiation, and cell cycle progression contributes to the advancement of MCE

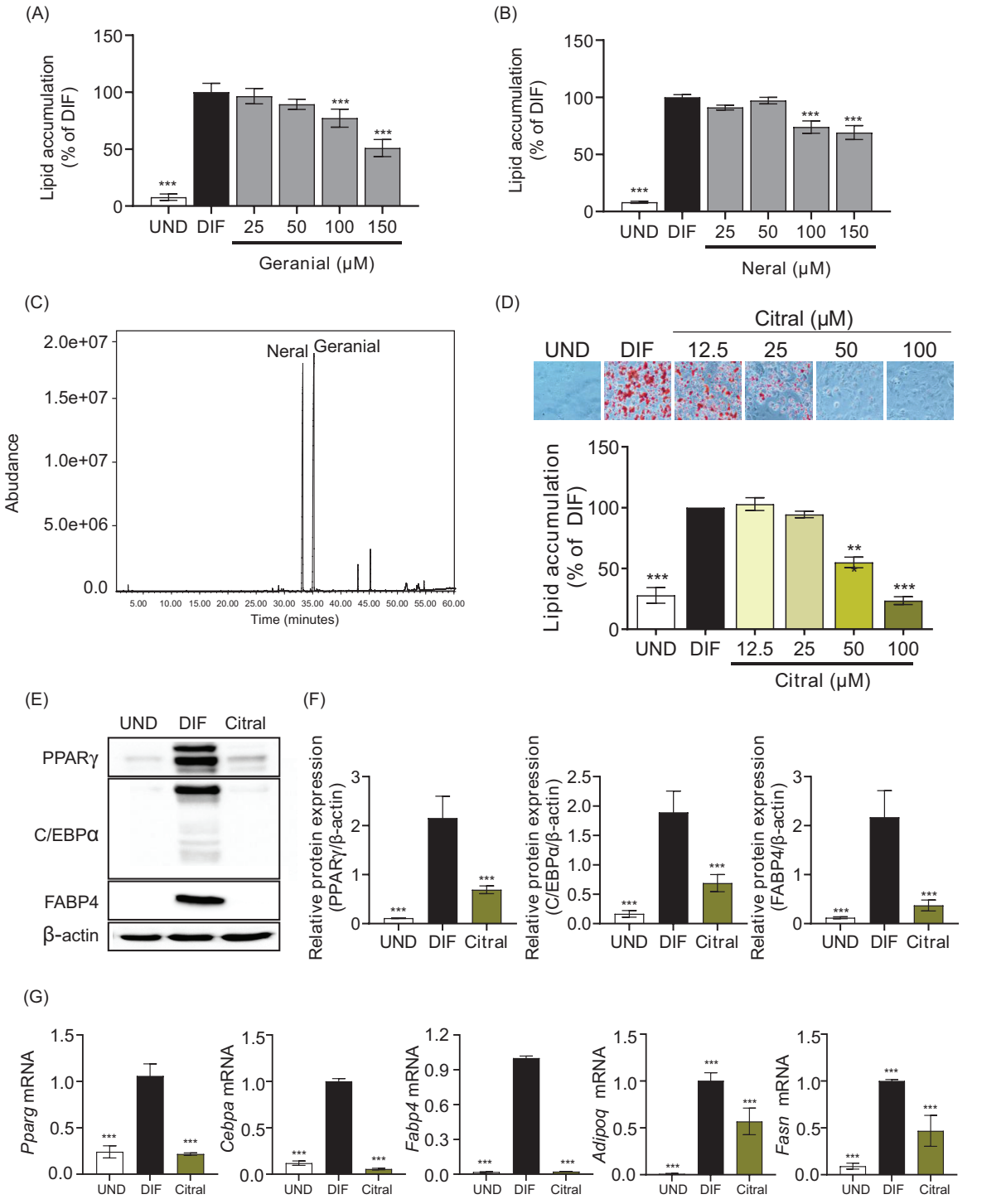

Figure 3. Inhibitory effect of citral on the differentiation of 3T3-L1 cells into adipocytes. (A and B) Changes in lipid accumulation during the differentiation of 3T3-L1 cells into adipocyte by (A) geranial and (B) neral. (C) GC-MS chromatogram of citral. (D) Inhibition of lipid accumulation by citral during the differentiation of preadipocytes into adipocyte. (E and F) The protein expression levels of adipogenic markers (*PPARγ*, *C/EBPα*, and *Fabp4*). (G) The mRNA expression levels of adipogenic markers (*Pparg*, *Cebpa*, and *Fabp4*), an adipokine marker (*Adipoq*) and a lipogenesis marker (*Fasn*) in citral-treated 3T3-L1 adipocytes. All data are presented as mean ± SD and analyzed with one-way ANOVA, compared with that from the DIF group (n ≥ 3, ***$p < 0.001$).

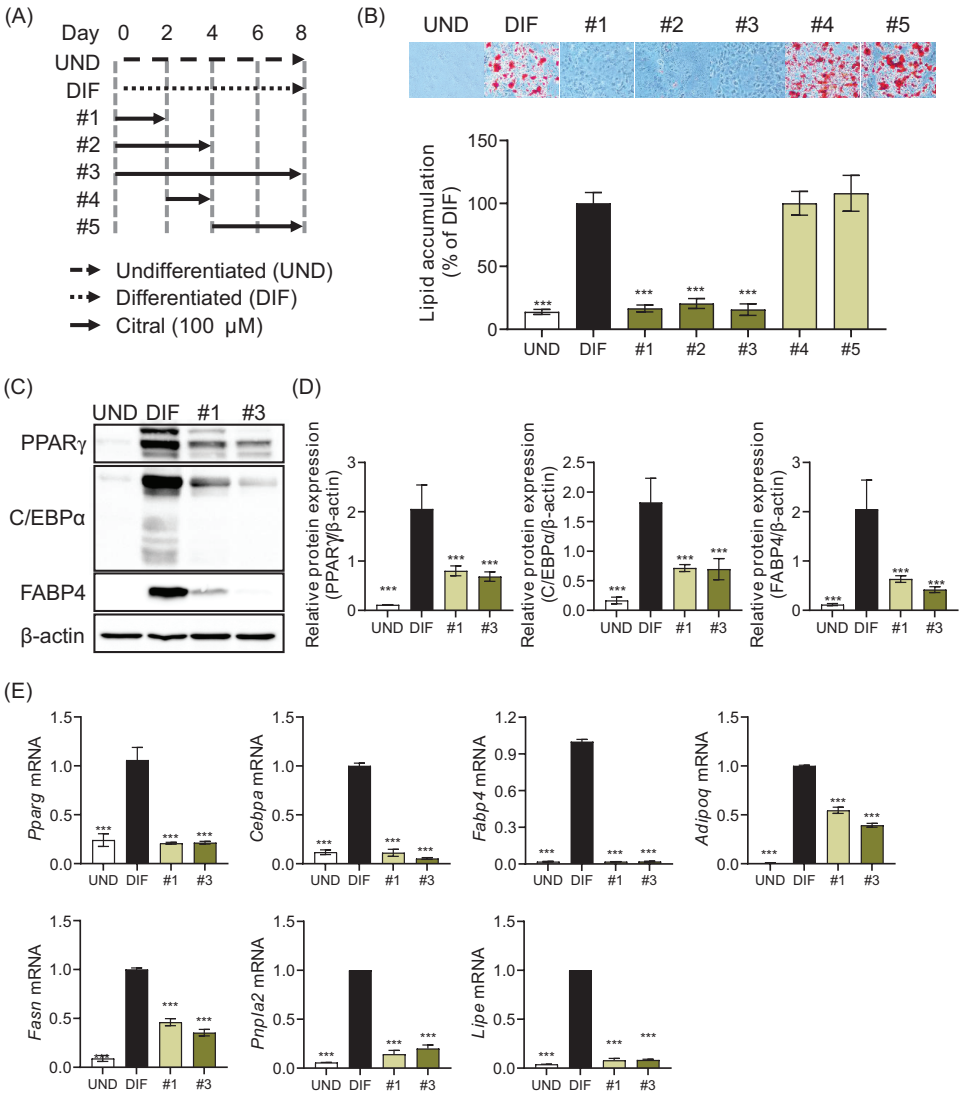

Figure 4. Anti-adipogenic effect of citral during the early stage of differentiation of 3T3-L1 cells by MDI. (A) Experimental scheme to evaluate the effects of citral treatments during the different stages of differentiation process. (B) Relative lipid accumulation measured by Oil Red O staining of 3T3-L1 cells treatment with citral for the indicated periods. (C and D) Comparison of protein expression levels of adipogenic markers and mRNA. (E) Expression levels of adipogenic markers, an adipokine marker, a lipogenesis marker, and lipolysis markers (*Pnpla2* and *Lipe*) in 3T3-L1 cells treated with citral for 0–2 (#1) and 0–8 days (#3). All data are presented as mean ± SD and analyzed with one-way ANOVA, compared with that from the DIF group. (n ≥ 3, ***$p < 0.001$).

(Tang *et al*., 2003b). Hence, we determined whether the anti-adipogenic effect of citral was related to MCE regulation, thereby inhibiting MDI-induced 3T3-L1 cell proliferation. MDI effectively increased the number of 3T3-L1 cells in the control group 48 h after treatment whereas almost no proliferation occurred in the citral-treated group (Figure 5A). Flow cytometry revealed that within 20 h, MDI induction led to typical cell cycle progression, transitioning from the G_0/G_1 phase to S and G_2/M phases. During this process, the percentage of cells in G_0/G_1 phase decreased from 79.0% to 46.5% whereas that in the S phase, it increased from 2.1% to 27.1% (Figure 5B). However, the proportion of cells in the S phase in citral-treated group was reduced by 5.6%, which suggests that citral may influence cell cycle dynamics and potentially delay the transition from G_0/G_1 phase to S phase. The protein and mRNA expressions of C/EBPβ, cyclins (cyclin D1, cycline E, and cyclin B1), and CDKs (CDK6 and CDK2) were also modified (Figures 5C–5E). MDI treatment enhanced the expression levels of C/EBPβ and biomarkers related to G1 phase (cyclin D1 and CDK6) and G_1/S boundary (cyclin E and CDK2) whereas citral treatment significantly suppressed those expression levels at 16 h and 20 h. Cyclin B1, a regulator of G_2/M phase, was highly

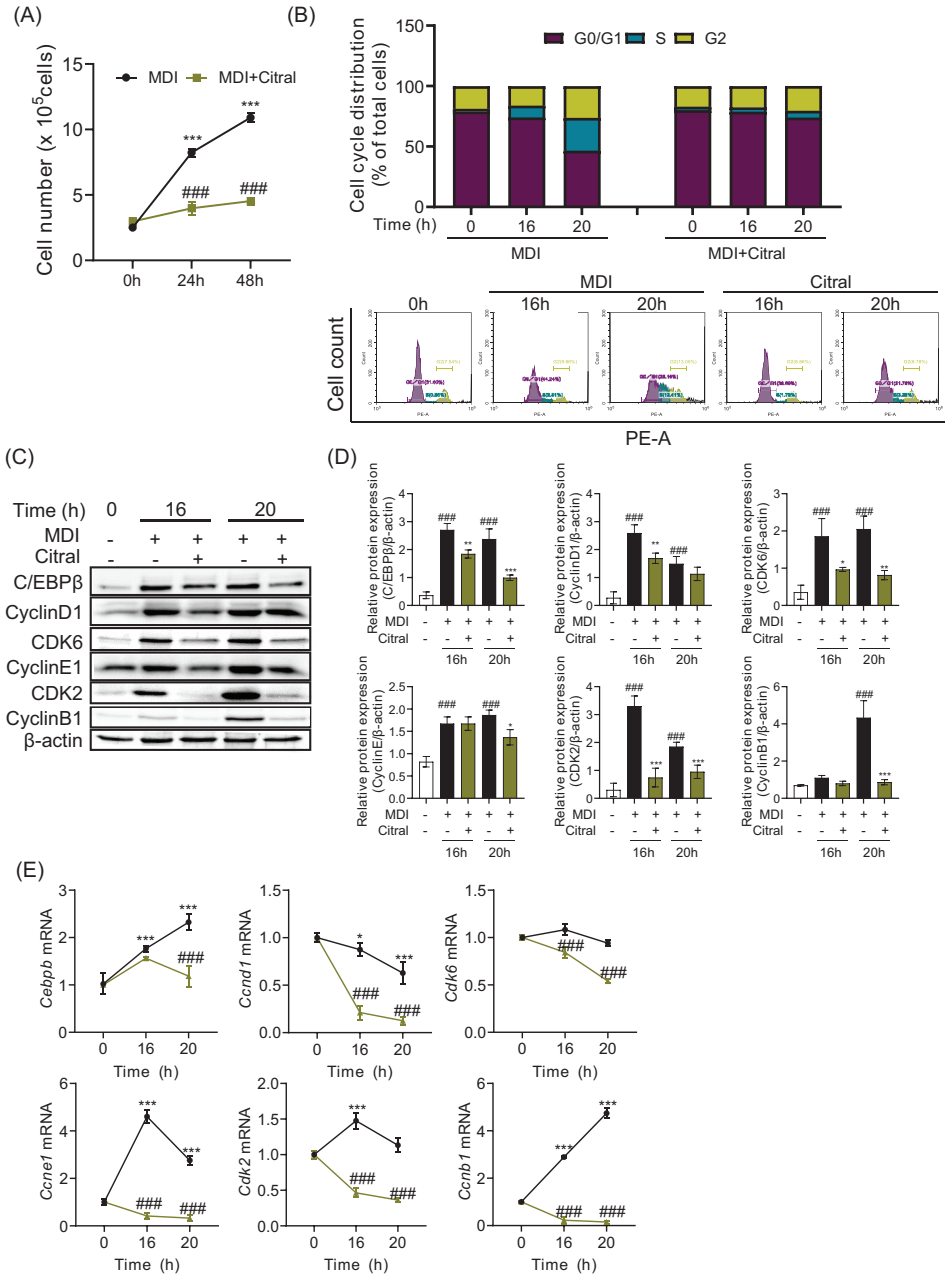

Figure 5. Effects of citral on cell cycle progression during mitotic clonal expansion (MCE) process. (A) Changes in the number of 3T3-L1 preadipocytes by citral after 24 and 48 h. (B) Changes in the phase distribution (G_0/G_1, S, and G_2/M phases) of cell cycle progression by citral. Each value of flow cytometry shown was derived by counting at least 10,000 events. The numbers of cells in G_0/G_1, S, and G_2/M phases are expressed as percentages of total cells. (C and D) Citral-induced time-dependent changes in protein and mRNA. (E) Expression levels of C/EBPβ and cell cycle phase markers (cyclin D1, CDK6, cyclin E, CDK2, and cyclin B1) in MDI-treated preadipocytes. The data are presented as mean ± SD (###$p < 0.001$ compared to the MDI group; ***$p < 0.001$ compared to MDI 0 h) from three independent experiments.

expressed in MDI-treated cells at 20 h but not expressed in citral-treated cells. Therefore, our results suggest that citral prevents cell cycle progression by arresting cells in the G_0/G_1 phase during the MCE of adipogenesis.

Mitotic clonal expansion is necessary to initiate differentiation of growth-arrested preadipocytes. Therefore, the inhibition of MCE can induce unbalanced differentiation (Tang *et al*., 2003a), and this effect has been studied for various food ingredients. Curcumin, a key bioactive compound found in the rhizomes of turmeric plant (*Curcuma longa*), suppresses adipogenic differentiation by inhibiting MCE during the early stages of adipocyte differentiation (Kim *et al*., 2011). Cell cycle progression

is delayed as transitions from G_1 to S phase and from S to G_2/M phase are reduced by curcumin. Sulforaphane, a compound naturally occurring in cruciferous vegetables, inhibits MCE by reducing C/EBPβ expression, arrests cell cycle at G_0/G_1 phase, increases protein p27 expression, and decreases retinoblastoma phosphorylation (Choi *et al*., 2012). Many flavor compounds also inhibit MCE. Carnosic acid, a major component of rosemary extract, attenuates the differentiation of adipocytes and arrests cell cycle entry into G_2/M phase by inhibiting C/EBPβ levels in 3T3-L1 cells (Gaya *et al*., 2013). β-Asarone, a major component of calamus oil, attenuates adipogenic master regulators and inhibits C/EBPβ expression (Lee *et al*., 2011). Cinnamon-derived aroma compounds, cinnam aldehyde and cinnamyl isobutyrate, suppress lipid accumulation by down-regulating C/EBPβ levels (Hoi *et al*., 2020). These compounds regulate the maturation of adipocytes during MCE, leading to a reduction in lipid accumulation and have potential benefits for obesity management. Consistent with these studies, citral inhibited adipogenesis by regulating adipogenic transcription factors and cell cycle pathways.

Effect of citral on Ak strain transforming (Akt) signaling in differentiation of 3T3-L1 cells

Mitotic clonal expansion progresses by activating several upper signaling pathways, including phosphatidylinositol 3-kinase–Akt (PI3K/Akt) and extracellular signal-regulated kinase (ERK), via hormonal inducers (Wen *et al*., 2022). Therefore, we investigated the upstream signaling cascades related to citral-induced MCE inhibition (Figure 6). MDI treatment strongly stimulated PI3K and Akt phosphorylation; however, citral treatment effectively decreased the MDI-induced Akt phosphorylation after 30 min. However, citral did not affect the ERK signaling pathway.

3T3-L1 differentiation is initiated by the hormonal inducer, MDI, which triggers the MCE stage. Prior to initiating cell cycle progression and activating a transcription factor cascade, MDI activates several signaling pathways, including Akt and ERK. Insulin, a component of MDI, binds to insulin receptor on cell surface, thereby initiating downstream signaling pathways, notably the PI3K/Akt pathway (Savova *et al*., 2023). Dexamethasone, another MDI component, activates the ERK pathway (Prusty *et al*., 2002). The PI3K/Akt pathway plays a crucial role in initiating MCE by supporting cell division and coordinating lipid accumulation whereas ERK primarily promotes cell proliferation during the early stages of MCE and indirectly contributes to differentiation. Both pathways stimulate cell proliferation, particularly in the early stages of adipocyte differentiation when cell expansion is required. Thus, the regulation of these pathways may influence MCE and, by extension, adipogenesis. Epigallocatechin gallate suppresses clonal expansion of adipocytes by significantly inhibiting the PI3K/Akt and mitogen-activated protein kinase kinase (MEK)/ERK

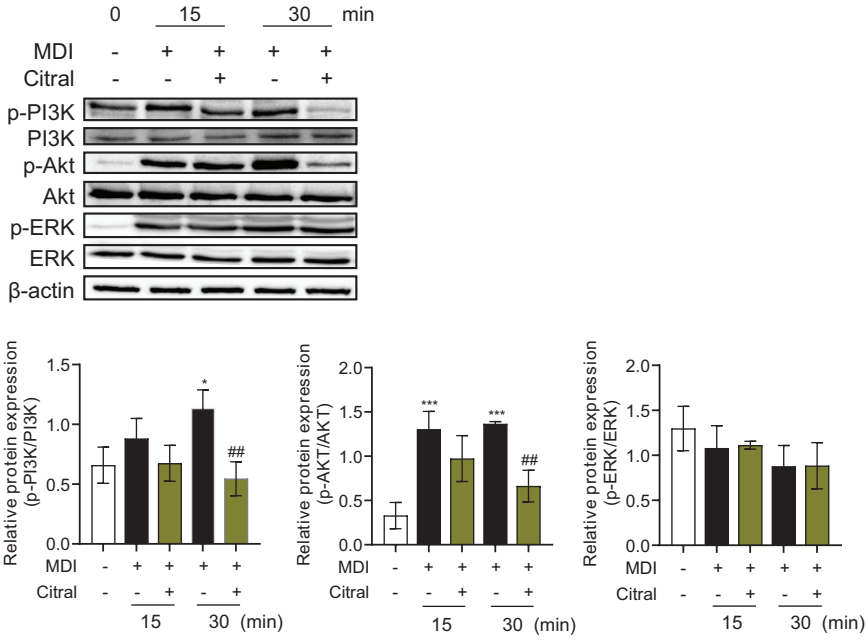

Figure 6. Effects of citral on PI3K/Akt singling pathway by Western blot analysis. The data are presented as mean ± SD (##p < 0.01, compared to the MDI group at the same time; *p < 0.05 and ***p < 0.001 compared to MDI, 0 h) from three independent experiments.

pathways (Kim and Sakamoto, 2012). The inhibition of a single pathway can influence adipogenesis. Piceatannol suppresses MCE by reducing the activation of insulin signaling pathway, which in turn inhibits the PI3K/Akt pathway during the early stages of adipogenesis (Kwon *et al*., 2012). Consistent with the results for piceatannol, citral was found to affect only the PI3K/Akt pathway. Collectively, citral suppressed the PI3K/Akt pathway among upstream signaling pathways, causing cell cycle arrest and inhibition of MCE progression, and was further shown to suppress adipogenesis.

Conclusions

In the present study, we demonstrated, for the first time, the potential anti-adipogenic effects of LMEO and its major components. Citral, a mixture of geranial and neral, was identified as the major component of LMEO by GC-MS, accounting for 88.67% of the total compounds in LMEO. The mechanism underlying the anti-adipogenic effects of citral was also identified. Citral down-regulates MDI-induced PI3K/Akt cellular signaling pathway, cell cycle progression, and adipogenesis-related transcription factors. Thus, the inhibitory effect of citral occurred through the inhibition of MCE, which is an early stage of adipogenesis. Our findings provide important insights into the mechanisms underlying the anti-obesity effects of citral. Citral and citral-enriched essential oils could potentially be used to prevent obesity, although it is important to note that further research and clinical trials are needed.

Data Availability

All data generated or analyzed during this study are included in this published article.

Acknowledgment

This study was supported by the Main Research Program (E0232201) of the Korea Food Research Institute (KFRI).

Author Contributions

Yae Rim Choi: investigation, formal analysis, and writing—original draft preparation. Min Kyung Park: investigation, formal analysis, and writing—review and editing. Ae Sin Lee: investigation and formal analysis. Young-Suk Kim: writing—review and editing. Min Jung Kim: conceptualization, methodology, supervision, writing—review and editing. All the authors approved the final version of the manuscript.

Competing interests

The authors declared no competing interests.

Conflict of Interests

The authors declare no conflict of interest.

Funding

This study was supported by the Main Research Program (E0232201) of the Korea Food Research Institute.

References

Ahmad, B., Serpell, C.J., Fong, I.L. and Wong, E.H. 2020. Molecular mechanisms of adipogenesis: the anti-adipogenic role of AMP-activated protein kinase. Front Mol Biosci. 7:76. https://doi.org/10.3389/fmolb.2020.00076

Araneda, R.C., Peterlin, Z., Zhang, X., Chesler, A. and Firestein, S. 2004. A pharmacological profile of the aldehyde receptor repertoire in rat olfactory epithelium. J Physiol. 555(Pt 3):743–756. https://doi.org/10.1113/jphysiol.2003.058040

Beikzadeh, S., Akbarinejad, A., Swift, S., Perera, J., Kilmartin, P.A. and Travas-Sejdic, J. 2020. Cellulose acetate electrospun nanofibers encapsulating lemon myrtle essential oil as active agent with potent and sustainable antimicrobial activity. React Function Polym. 157:104769. https://doi.org/10.1016/j.reactfunctpolym.2020.104769

Chang, E. and Kim, C.Y. 2019. Natural products and obesity: a focus on the regulation of mitotic clonal expansion during adipogenesis. Molecules. 24(6):1157. https://doi.org/10.3390/molecules24061157

Choi, K.M., Lee, Y.S., Sin, D.M., Lee, S., Lee, M.K., Lee, Y.M., Hong, T.J., Yun, Y.P., Yoo, H.S. 2012. Sulforaphane inhibits mitotic clonal expansion during adipogenesis through cell cycle arrest. Obesity (Silver Spring). 20(7):1365–1371. https://doi.org/10.1038/oby.2011.388

Chung, M.J., Cho, S.Y., Bhuiyan, M.J., Kim, K.H. and Lee, S.J. 2010. Anti-diabetic effects of lemon balm (Melissa officinalis) essential oil on glucose- and lipid-regulating enzymes in type 2 diabetic mice. Br J Nutr. 104(2):180–188. https://doi.org/10.1017/s0007114510001765

Gaya, M., Repetto, V., Toneatto, J., Anesini, C., Piwien-Pilipuk, G. and Moreno, S. 2013. Antiadipogenic effect of carnosic acid, a natural compound present in *Rosmarinus officinalis*, is exerted through the C/EBPs and PPARγ pathways at the onset of the differentiation program. Biochim Biophys Acta. 1830(6):3796–3806. https://doi.org/10.1016/j.bbagen.2013.03.021

Geary, N. 2013. Understanding synergy. Am J Physiol Endocrinol Metab. 304(3):E237–E253. https://doi.org/10.1152/ajpendo.00308.2012

Ghasemi Pirbalouti, A., Nekoei, M., Rahimmalek, M. and Malekpoor, F. 2019. Chemical composition and yield of essential

oil from lemon balm (*Melissa officinalis* L.) under foliar applications of jasmonic and salicylic acids. Biocataly Agric Biotechnol. 19:101144. https://doi.org/10.1016/j.bcab.2019.101144

Gonçalves, E.C.D., Assis, P.M., Junqueira, L.A., Cola, M., Santos, A.R.S., Raposo, N.R.B. and Dutra, R.C. 2020. Citral inhibits the inflammatory response and hyperalgesia in mice: the role of TLR4, TLR2/Dectin-1, and CB2 cannabinoid receptor/ATP-sensitive K+ channel pathways. J Nat Prod. 83(4):1190–1200. https://doi.org/10.1021/acs.jnatprod.9b01134

Guo, L., Li, X. and Tang, Q.Q. 2015. Transcriptional regulation of adipocyte differentiation: a central role for CCAAT/enhancer-binding protein (C/EBP) β. J Biol Chem. 290(2):755–761. https://doi.org/10.1074/jbc.R114.619957

Harada, N., Ishihara, M., Horiuchi, H., Ito, Y., Tabata, H., Suzuki, Y. A., Nakano, Y., Yamaji, R., Inui, H. 2016. Mogrol derived from siraitia grosvenorii mogrosides suppresses 3T3-L1 adipocyte differentiation by reducing cAMP-response element-binding protein phosphorylation and increasing AMP-activated protein kinase phosphorylation. PLoS One. 11(9):e0162252. https://doi.org/10.1371/journal.pone.0162252

Hoi, J.K., Lieder, B., Liebisch, B., Czech, C., Hans, J., Ley, J.P. and Somoza, V. 2020. TRPA1 agonist cinnamaldehyde decreases adipogenesis in 3T3-L1 cells more potently than the non-agonist structural analog cinnamyl isobutyrate. ACS Omega. 5(51):33305–33313. https://doi.org/10.1021/acsomega.0c05083

Jain, N. and Sharma, M. 2017. Evaluation of citrus lemon essential oil for its chemical and biological properties against fungi causing dermatophytic infection in human beings. Anal Chem Lett. 7(3):402–409. https://doi.org/10.1080/22297928.2017.1349620

Kang, S.I., Ko, H.C., Shin, H.S., Kim, H.M., Hong, Y.S., Lee, N.H. and Kim, S.J. 2011. Fucoxanthin exerts differing effects on 3T3-L1 cells according to differentiation stage and inhibits glucose uptake in mature adipocytes. Biochem Biophys Res Commun. 409(4):769–774. https://doi.org/10.1016/j.bbrc.2011.05.086

Kim, M.A., Kang, K., Lee, H.J., Kim, M., Kim, C.Y. and Nho, C.W. 2014. Apigenin isolated from Daphne genkwa siebold et zucc. inhibits 3T3-L1 preadipocyte differentiation through a modulation of mitotic clonal expansion. Life Sci. 101(1–2):64–72. https://doi.org/10.1016/j.lfs.2014.02.012

Kim, C.Y., Le, T.T., Chen, C., Cheng, J.-X. and Kim, K.-H. 2011. Curcumin inhibits adipocyte differentiation through modulation of mitotic clonal expansion. J Nutr Biochem. 22(10):910–920. https://doi.org/10.1016/j.jnutbio.2010.08.003

Kim, G.S., Park, H.J., Woo, J.H., Kim, M.K., Koh, P.O., Min, W., Ko, Y.G., Kim, C.H., Won, C.K., Cho, J.H. 2012. Citrus aurantium flavonoids inhibit adipogenesis through the Akt signaling pathway in 3T3-L1 cells. BMC Complement Altern Med. 12:31. https://doi.org/10.1186/1472-6882-12-31

Kim, H. and Sakamoto, K. 2012. (-)-Epigallocatechin gallate suppresses adipocyte differentiation through the MEK/ERK and PI3K/Akt pathways. Cell Biol Int. 36(2):147–153. https://doi.org/10.1042/cbi20110047

Kwon, J.Y., Seo, S.G., Heo, Y.S., Yue, S., Cheng, J.X., Lee, K.W. and Kim, K.H. 2012. Piceatannol, natural polyphenolic stilbene, inhibits adipogenesis via modulation of mitotic clonal expansion and insulin receptor-dependent insulin signaling in early phase of differentiation. J Biol Chem. 287(14):11566–11578. https://doi.org/10.1074/jbc.M111.259721

Lee, M.-H., Chen, Y.-Y., Tsai, J.-W., Wang, S.-C., Watanabe, T. and Tsai, Y.-C. 2011. Inhibitory effect of β-asarone, a component of *Acorus calamus* essential oil, on inhibition of adipogenesis in 3T3-L1 cells. Food Chem. 126(1):1–7. https://doi.org/10.1016/j.foodchem.2010.08.052

Liao, P.-C., Yang, T.-S., Chou, J.-C., Chen, J., Lee, S.-C., Kuo, Y.-H., Ho, C.-L., Chao, L. K.-P. 2015. Anti-inflammatory activity of neral and geranial isolated from fruits of Litsea cubeba Lour. J Func Foods. 19:248–258. https://doi.org/10.1016/j.jff.2015.09.034

Lim, A.C., Tang, S.G.H., Zin, N.M., Maisarah, A.M., Ariffin, I.A., Ker, P.J. and Mahlia, T.M.I. 2022. Chemical composition, antioxidant, antibacterial, and antibiofilm activities of *Backhousia citriodora* essential oil. Molecules. 27(15):4895. https://doi.org/10.3390/molecules27154895

Longo, M., Zatterale, F., Naderi, J., Parrillo, L., Formisano, P., Raciti, G. A., Befuinot, F., Miele, C. 2019. Adipose tissue dysfunction as determinant of obesity-associated metabolic complications. Int J Mol Sci. 20(9):2358. https://doi.org/10.3390/ijms20092358

Mercer, D.G. and Rodriguez-Amaya, D.B. 2021. Reactions and interactions of some food additives, Chap. 12. In: Rodriguez-Amaya, D.B. and Amaya-Farfan, J. (Eds.) Chemical Changes During Processing and Storage of Foods. Academic Press, Cambridge, MA, pp. 579–635.

Modak, T. and Mukhopadhaya, A. 2011. Effects of citral, a naturally occurring antiadipogenic molecule, on an energy-intense diet model of obesity. Indian J Pharmacol. 43(3):300–305. https://doi.org/10.4103/0253-7613.81515

Moseti, D., Regassa, A. and Kim, W.K. 2016. Molecular regulation of adipogenesis and potential anti-adipogenic bioactive molecules. Int J Mol Sci. 17(1):124. https://doi.org/10.3390/ijms17010124

Mukarram, M., Choudhary, S., Khan, M.A., Poltronieri, P., Khan, M.M.A., Ali, J., Kurjak, D. Shahid, M. 2021. Lemongrass essential oil components with antimicrobial and anticancer activities. Antioxidants (Basel). 11(1):20. https://doi.org/10.3390/antiox11010020

Niijima, A. and Nagai, K. 2003. Effect of olfactory stimulation with flavor of grapefruit oil and lemon oil on the activity of sympathetic branch in the white adipose tissue of the epididymis. *Exp Biol Med (Maywood):228*(10):1190–1192. https://doi.org/10.1177/153537020322801014

Nordin, N., Yeap, S.K., Rahman, H.S., Zamberi, N.R., Mohamad, N.E., Abu, N., Masarudin, M.J., Abdullah, R., Alitheen, N.B. 2020. Antitumor and anti-metastatic effects of citral-loaded nanostructured lipid carrier in 4T1-induced breast cancer mouse model. Molecules. 25(11):2670. https://doi.org/10.3390/molecules25112670

Patel, Y.M. and Lane, M.D. 2000. Mitotic clonal expansion during preadipocyte differentiation: calpain-mediated turnover of p27. J Biol Chem. 275(23):17653–17660. https://doi.org/10.1074/jbc.M910445199

Prusty, D., Park, B.H., Davis, K.E. and Farmer, S.R. 2002. Activation of MEK/ERK signaling promotes adipogenesis by enhancing peroxisome proliferator-activated receptor gamma

(PPAR gamma) and C/EBP alpha gene expression during the differentiation of 3T3-L1 preadipocytes. J Biol Chem. 277(48):46226–46232. https://doi.org/10.1074/jbc.M207776200

Qiu, Z., Wei, Y., Chen, N., Jiang, M., Wu, J. and Liao, K. 2001. DNA synthesis and mitotic clonal expansion is not a required step for 3T3-L1 preadipocyte differentiation into adipocytes. J Biol Chem. 276(15):11988–11995. https://doi.org/10.1074/jbc.M011729200

Rosen, E.D., Hsu, C.H., Wang, X., Sakai, S., Freeman, M.W., Gonzalez, F.J. and Spiegelman, B.M. 2002. C/EBPalpha induces adipogenesis through PPAR gamma: a unified pathway. Genes Dev. 16(1):22–26. https://doi.org/10.1101/gad.948702

Rosen, E.D. and Spiegelman, B.M. 2000. Molecular regulation of adipogenesis. Annu Rev Cell Dev Biol. 16:145–171. https://doi.org/10.1146/annurev.cellbio.16.1.145

Savova, M.S., Mihaylova, L.V., Tews, D., Wabitsch, M. and Georgiev, M.I. 2023. Targeting PI3K/AKT signaling pathway in obesity. Biomed Pharmacother. 159:114244. https://doi.org/https://doi.org/10.1016/j.biopha.2023.114244

Shi, C., Song, K., Zhang, X., Sun, Y., Sui, Y., Chen, Y., Jia, Z., Sun, H., Sun, Z., Xia, X. 2016. Antimicrobial activity and possible mechanism of action of citral against *Cronobacter sakazakii*. PLoS One. 11(7):e0159006. https://doi.org/10.1371/journal.pone.0159006

Soliman, W.S., Salaheldin, S. and Amer, H.M. 2017. Chemical composition evaluation of Egyptian lemongrass, Cymbopogon citratus, essential oil. Int J Sci Eng Res. 8(11):630–634.

Southwell, I. 2021. *Backhousia citriodora* F. Muell. (lemon myrtle): an unrivalled source of citral. Foods. 10(7):1596. https://doi.org/ARTN159610.3390/foods10071596

Sprenger, S., Woldemariam, T., Kotchoni, S., Elshabrawy, H.A. and Chaturvedi, L.S. 2022. Lemongrass essential oil and its major constituent citral isomers modulate adipogenic gene expression in 3T3-L1 cells. J Food Biochem. 46(2):e14037. https://doi.org/10.1111/jfbc.14037

Sri Devi, S. and Ashokkumar, N. 2018. Citral, a monoterpene inhibits adipogenesis through modulation of adipogenic transcription factors in 3T3-L1 cells. Indian J Clin Biochem. 33(4):414–421. https://doi.org/10.1007/s12291-017-0692-z

Sultanbawa, Y. 2016. Lemon myrtle (*Backhousia citriodora*) oils, Chap. 59. In: Preedy, V.R. (Ed.) Essential Oils in Food Preservation, Flavor and Safety. Academic Press, San Diego, CA, pp. 517–521.

Tang, Q.-Q., Otto, T.C. and Lane, M.D. 2003a. CCAAT/enhancer-binding protein β is required for mitotic clonal expansion during adipogenesis. Proc Nat Acad Sci. 100(3):850–855. https://doi.org/10.1073/pnas.0337434100

Tang, Q.-Q., Otto, T.C. and Lane, M.D. 2003b. Mitotic clonal expansion: a synchronous process required for adipogenesis. Proc Natl Acad Sci. 100(1):44–49. https://doi.org/10.1073/pnas.0137044100

Wang, Y.F., Zheng, Y., Cha, Y.Y., Feng, Y., Dai, S.X., Zhao, S., Chen, H., Xu, M. 2023. Essential oil of lemon myrtle (*Backhousia citriodora*) induces S-phase cell cycle arrest and apoptosis in HepG2 cells. J Ethnopharmacol. 312:116493. https://doi.org/10.1016/j.jep.2023.116493

Wen, X., Zhang, B., Wu, B., Xiao, H., Li, Z., Li, R., Xu, X. andLi, T. 2022. Signaling pathways in obesity: mechanisms and therapeutic interventions. Signal Trans Target Ther. 7(1):298. https://doi.org/10.1038/s41392-022-01149-x

Yu, H.S., Kim, W.J., Bae, W.Y., Lee, N.K. and Paik, H.D. 2020. Inula britannica inhibits adipogenesis of 3T3-L1 preadipocytes via modulation of mitotic clonal expansion involving ERK 1/2 and Akt signaling pathways. Nutrients. 12(10):3037. https://doi.org/10.3390/nu12103037

Zeng, S., Kapur, A., Patankar, M.S. and Xiong, M.P. 2015. Formulation, characterization, and antitumor properties of trans-and cis-citral in the 4T1 breast cancer xenograft mouse model. Pharm Res. 32:2548–2558. https://doi.org/10.1007/s11095-015-1643-0

Zhang, H.J., Ji, B.P., Chen, G., Zhou, F., Luo, Y.C., Yu, H.Q., Gao, F.Y., Zhang, Z.P., Li, H.Y. 2009. A combination of grape seed-derived procyanidins and gypenosides alleviates insulin resistance in mice and HepG2 cells. J Food Sci. 74(1):H1–H7. https://doi.org/10.1111/j.1750-3841.2008.00976.x

Zhu, X., Yang, L., Xu, F., Lin, L. and Zheng, G. 2017. Combination therapy with catechins and caffeine inhibits fat accumulation in 3T3-L1 cells. Exp Ther Med. 13(2):688–694. https://doi.org/10.3892/etm.2016.3975